Displacement-Induced Switching Rates of Bioresponsive Hydrogel Microlenses

Jongseong Kim, Neetu Singh, and L. Andrew Lyon*

School of Chemistry and Biochemistry & Petit Institute for Bioengineering and Bioscience, Georgia Institute of Technology, Atlanta, Georgia 30332-0400

Received December 28, 2006. Revised Manuscript Received February 27, 2007

We report investigations of the response rates of bioresponsive hydrogel microlenses in order to gain a deeper understanding of their potential utility as a new label-free biosensing construct. Bioresponsive microgels were prepared from multi-responsive poly(*N*-isopropylacrylamide-*co*-acrylic acid) (pNIPAm-AAc) microgels after conjugation with biotin (as a bound target) and aminobenzophenone (ABP) (as a photoaffinity label) via carbodiimide chemistry. Bioresponsive hydrogel microlenses were then formed from individual microgels via Coulombic assembly of the anionic microgels onto a positively charged glass substrate. Incubation with polyclonal anti-biotin resulted in antibody-cross-linked microlenses. The antibodies were then photoligated to the hydrogel network via UV irradiation, making the microlenses reversibly sensitive to free biocytin by disruption of biotin−antibiotin binding. The response rates of the microlenses to biocytin binding (bound antibody−antigen displacement) were studied by monitoring the microlens optical properties via brightfield optical microscopy. The response rates of the hydrogel microlenses are strongly coupled to analyte concentrations at an equilibrium number of antigen−antibody binding on the hydrogel microlenses. These results suggest that the hydrogel microlens construct may be a potential candidate for label-free biosensing/bioassay of protein and small molecules.

Introduction

Recent efforts in the field of responsive materials have focused on the design of structures that respond to various stimuli. In particular, "bioresponsive" materials may allow for the design of systems that can be triggered to carry out a task or set of tasks in response to a biological event or stimulus. For example, drug delivery devices have been developed wherein drug release is coupled to a change in hydrogel structure, where that structural change is in turn coupled to the enzymatic cleavage of hydrogel cross-links.[1] A more simplistic construct would be one in which the material simply reports on the presence of a specific biomolecule, as in a bioanalytical application.[2−6] Our group has tackled this problem by using hydrogel microstructures to create bioresponsive materials. Overall, hydrogels represent an attractive scaffolding onto which bioresponsivity can be added, as hydrogels are traditionally a useful base material for both bioanalytical tools and biomaterials.[6−13]

The means by which a hydrogel can respond to a stimulus arise from the main controlling factors in hydrogel swelling. By changing one or more of these factors, which include the polymer hydrophilicity, network elasticity, and charge density (for polyelectrolyte hydrogels), one can cause the hydrogel to undergo a change in its equilibrium swelling.[14−17] In our approach, which has also been pursued by others for macroscopic gels,[4,5] we have coupled the elasticity (or cross-link density) of the *outer surface* of a hydrogel microparticle (microgel) to an antibody−antigen association−dissociation equilibrium. In the bound state, the degree of cross-linking at the microgel surface is increased, resulting in hydrogel deswelling at the surface. In the presence of soluble antigen, the bound antibody−antigen cross-link is disrupted, resulting in swelling at the microgel−solution interface.[18] In this fashion, we have coupled the thermodynamics of gel swelling to the thermodynamics of antibody−antigen (or protein−ligand) binding, thereby providing a generalizable platform into which a broad range of different bioresponsivities can

* To whom correspondence should be addressed: e-mail LL62@mail.gatech.edu.

(1) Tauro, J. R.; Gemeinhart, R. A. *Bioconjugate Chem.* **2005**, *16*, 1133−1139.
(2) Kim, J.; Nayak, S.; Lyon, L. A. *J. Am. Chem. Soc.* **2005**, *127*, 9588−9592.
(3) Sharma, A. C.; Jana, T.; Kesavamoorthy, R.; Shi, L.; Virji, M. A.; Finegold, D. N.; Asher, S. A. *J. Am. Chem. Soc.* **2004**, *126*, 2971−2977.
(4) Miyata, T.; Jige, M.; Nakaminami, T.; Uragami, T. *Proc. Natl. Acad. Sci. U.S.A.* **2006**, *103*, 1190−1193.
(5) Miyata, T.; Asami, N.; Uragami, T. *Nature* **1999**, *399*, 766−769.
(6) Ehrick, J. D.; Deo, S. K.; Browning, T. W.; Bachas, L. G.; Madou, M. J.; Daunert, S. *Nat. Mater.* **2005**, *4*, 298−302.
(7) Nayak, S.; Lyon, L. A. *Angew. Chem., Int. Ed.* **2004**, *43*, 6706−6709.
(8) Nayak, S.; Lee, H.; Chmielewski, J.; Lyon, L. A. *J. Am. Chem. Soc.* **2004**, *126*, 10258−10259.
(9) Kim, S.; Healy, K. E. *Biomacromolecules* **2003**, *4*, 1214−1223.
(10) Lutolf, M. P.; Lauer-Fields, J. L.; Schmoekel, H. G.; Metters, A. T.; Weber, F. E.; Fields, G. B.; Hubbell, J. A. *Proc. Natl. Acad. Sci. U.S.A.* **2003**, *100*, 5413−5418.
(11) Jeong, B.; Bae, Y. H.; Lee, D. S.; Kim, S. W. *Nature* **1997**, *388*, 860−862.
(12) Luo, Y.; Shoichet, M. S. *Nat. Mater.* **2004**, *3*, 249−253.
(13) Qiu, Y.; Park, K. *Adv. Drug Delivery Rev.* **2001**, *53*, 321−339.
(14) Dusek, K.; Patterson, K. *J. Polym. Sci., Polym. Phys. Ed.* **1968**, *6*, 1209−16.
(15) Tanaka, T.; Fillmore, D. J. *J. Chem. Phys.* **1979**, *70*, 1214−1218.
(16) Tanaka, T.; Fillmore, D. J.; Sun, S.-T.; Nishio, I.; Swislow, G.; Shah, A. *Phys. Rev. Lett.* **1980**, *45*, 1636−1639.
(17) Pelton, R. *Adv. Colloid Interface Sci.* **2000**, *85*, 1−33.
(18) Kim, J.; Singh, N.; Lyon, L. A. *Angew. Chem. Int. Ed.* **2006**, *45*, 1446−1449.

10.1021/cm063086p CCC: $37.00
Published on Web 04/17/2007

potentially be engineered. Furthermore, by localization of the binding to the microgel surface only, hydrogel swelling will be more rapid than methods in which diffusion of the analyte throughout the bulk of the gel is required, as is the case with macroscopic bioresponsive gels.[4,5] Finally, it is expected that surface-based binding may result in a more reversible construct, as the chances of irreversible entrapment of analyte within the bulk of the network should be reduced.

In this paper we present an investigation into the response rates of bioresponsive hydrogel microlenses exposed to a range of concentrations of analyte (biocytin, a water-soluble biotin analogue). The measurement of response rates is important for two main reasons. First, because the response of the sensor is dependent on antibody−antigen displacement, it is possible that such an approach could be too sluggish to be practically applicable in a sensing application. For example, displacement-based immunoassays are often subjected to long (8−12 h) incubations in order to attain equilibrium. This would obviously not be useful for many sensing approaches. Second, we have proposed in our previous work that the bioresponsive microlens construct is one that relies on the interplay between antibody−antigen binding thermodynamics and gel swelling thermodynamics. Such an interplay should be clearly reflected by a change in the characteristic time scales for displacement as a function of the number of antibody−antigen interactions as well as the solution concentration of free antigen. The results presented below support this hypothesis.

As in our previous publications,[2,18−21] we use microlensing as a convenient method for determining the degree of microgel swelling, as this is much simpler and more rapid than determining the actual three-dimensional size changes of the surface-bound microgel. Our efforts in this regard have involved studies of the initial formation of substrate-supported microlenses,[20] determination of the temperature/pH responsivity of simple microlenses,[21] fabrication of photoresponsive microlens arrays,[19] measurement of direct protein binding to ligand-functionalized microlenses,[2] and development of reversible bioresponsive microlenses.[18] In all of these studies, the microgel is adsorbed to a silane-modified glass substrate, where it deforms into a plano-convex structure. The focusing power of this microlens, which is related to the degree of surface deswelling, can then be determined by projection of an image through the microlens. An optical microscope can conveniently be used for both image projection and visualization.

Experimental Section

Materials. All reagents were purchased from Sigma−Aldrich unless otherwise specified. The monomer *N*-isopropylacrylamide (NIPAm) was recrystallized from hexanes (J.T. Baker) prior to use. The cross-linker *N*,*N*′-methylenebisacrylamide (BIS) and the initiator ammonium persulfate (APS) were used without further purification. Acrylic acid (AAc) was distilled under reduced pressure. The glass coverslips used as substrates were 24 × 50 mm Fisher Finest brand cover glass. The cationic silane 3-aminopropyltrimethoxysilane (APTMS) was used for functionalization of the glass substrates. Absolute (200 proof) and 95% ethanol were used for various purposes in this investigation. The water-soluble carbodiimide 1-ethyl-3-(3-dimethylaminopropyl)carbodiimide (EDC) and biotin hydrazide were purchased from Pierce. Dimethyl sulfoxide (DMSO) was obtained from J.T. Baker. Polyclonal anti-biotin (raised in goat) was purchased from Sigma−Aldrich. Water was distilled and then deionized (DI) to a resistance of at least 18 MΩ (Barnstead Thermolyne E-Pure system) and then filtered through a 0.2 μm filter to remove particulate matter before use. For printing the projection pattern, 3M transparency film and a Hewlett-Packard LaserJet 4000N printer were used.

Methods: *1. Microgel Synthesis and Functionalization.* Bioresponsive microgels were prepared by free-radical precipitation polymerization of NIPAm. Acrylic acid was used as a comonomer to incorporate carboxyl functional groups for further biofunctionalization. For the synthesis, reactant mixture composed of a total monomer concentration of 300 mM with a molar composition of 89.4% NIPAm and 0.5% BIS (cross-linker), was made by dissolving the monomers in 100 mL of deionized water. The reactant mixture was filtered through a 0.8 μm filter and then transferred into a 250 mL three-neck round-bottom flask. During 60 min of N_2 purge, the mixture was heated to 70 °C and maintained at the same temperature throughout the synthesis. Comonomers AAc (10%) and 4-acrylamidofluorescein (0.1%) were added to the reaction mixture. After addition of the comonomers, 1 mL of 6.13 mM APS was added to initiate the polymerization process. The copolymerization was allowed to proceed for 4 h at 70 °C under N_2. The resultant colloidal dispersion was dialyzed against water for ∼2 weeks, with the water being changed twice per day, by use of 10 000 MW cutoff dialysis tubing (VWR).

For biotinylation of the AAc carboxyl groups, the pNIPAm-AAc microgel solution was diluted 10-fold with 2-[*N*-morpholino]-ethanesulfonic acid (MES) buffer (pH 4.7). Biotin hydrazide (3.8 mg dissolved in 0.5 mL of DMSO) was then added to 1 mL of dilute microgel solution (10% v/v dilution of initial concentration following synthesis), followed by the addition of 15 mg of EDC. The reaction was kept overnight at 4 °C while stirring. Unreacted biotin hydrazide was removed by several cycles of centrifugation followed by resuspension of the microgel pellet in phosphate-buffered saline (PBS) (pH 7.5).

In order to covalently couple the antigen-bound antibody to the microlenses to form a reversible cross-link, a photoaffinity approach is used.[18] Aminobenzophenone (ABP) is coupled to the particles and then can be used to affect photoattachment of the antibodies once they have assembled (via antigen binding) on the microlens surface. Without this step, the antibodies would simply diffuse off the microlens surface once they were displaced with free antigen. We have also shown previously that the ABP present on the microlenses, which is confined between the microlens and the silanized glass substrate following deposition, can be used to covalently couple the microlenses to the glass.[18] This provides for a more robust sensor design. For the modification of the biotinylated pNIPAm-AAc particles with ABP, the biotinylated microgel particle solution (1 mL) was centrifuged five times and the resulting white pellet was redispersed in 700 μL of DMSO. To this was added 150 μL each of 0.01 M ABP and 0.01 M *N*,*N*′-dicyclohexylcarbodiimide (DCC) solution in DMSO. The reaction solution was stirred overnight at room temperature in the dark, following which 0.5 mL of deionized water was added. The white solid precipitate of *N*,*N*′-dicyclohexylurea thus formed was filtered off. The resultant filtrate was centrifuged at 14 000 rpm for 15 min and the pellet

(19) Kim, J.; Serpe, M. J.; Lyon, L. A. *Angew. Chem., Int. Ed. Engl.* **2005**, *44*, 1333−1336.
(20) Serpe, M. J.; Kim, J.; Lyon, L. A. *Adv. Mater.* **2004**, *16*, 184−187.
(21) Kim, J.; Serpe, M. J.; Lyon, L. A. *J. Am. Chem. Soc.* **2004**, *126*, 9512−9513.

was redispersed in DMSO, followed by four additional centrifugation cycles and redispersion in PBS buffer (pH 7.5). Note that the synthetic scheme employs a stoichiometric amount of biotin and ABP for coupling with the carboxyl groups. Also, the reaction efficiency of the carbodiimide coupling is <100%; hence the unreacted carboxyl groups can be further used for binding to the cationic glass substrate.

2. Bioresponsive Hydrogel Microlens Substrate Preparation. Glass coverslips were treated in an Ar plasma (Harrick Scientific) for 30 min to remove any organic residuals from the glass surface. Plasma treatment was followed by immersion of the glass substrates in an ethanolic (absolute ethanol) 1% APTMS solution for ~2 h, after which they were removed from the solution and rinsed several times with 95% ethanol. These silane-functionalized glass substrates were stored in 95% ethanol for no longer than 5 days prior to use. Prior to microgel assembly, the substrates were rinsed with DI water and dried by a stream of N_2 gas. The silane-functionalized glass substrate was then exposed to an aqueous biotin/ABP functionalized microgel solution buffered by 10 mM PBS, pH 7.5. After 30 min, the substrate was rinsed with DI water and dried with N_2 gas to leave behind microgels that are strongly attached to the substrate via Coulombic interactions. Note that nonfunctionalized microgels are also attached to the substrate in similar way as an internal (nonbioresponsive) reference. A microlens array/silicone gasket/coverslip sandwich assembly was prepared, and then a solution of polyclonal anti-biotin diluted with pH 7.5 PBS was introduced into the void space. After 3 h of antibody incubation, the substrate was rinsed and the medium was replaced with pH 7.5 PBS. The antigen-bound antibody was photoligated and, thereby, cross-linked to the microgel network by the microgel-tethered ABP via irradiation with a 100 W long-wave UV lamp for 30 min while the coverslip was cooled on an ice bath.[22] Various biocytin concentrations (60 μL aliquots) buffered in 10 mM PBS were introduced into the void space of the assembly for microscopic investigations of competitive antigen−antibody binding.

3. Microscopy. Brightfield transmission and differential interference contrast (DIC) optical microscopies were used to study the changes in the optical properties of the hydrogel microlens attached to the substrate. An Olympus IX70 inverted microscope equipped with a high numerical aperture, oil immersion 100× objective (NA = 1.30) was used for all microscopies reported here. Images were captured by use of a black/white charge-coupled device (CCD) camera (PixelFly, Cooke Corp.). The microscope setup used in this experiment is shown in Scheme 1.

Results and Discussion

The main purpose of this study is to investigate the response rate of the bioresponsive hydrogel microlenses. To accomplish this goal, we prepared a bioresponsive hydrogel microlens construct containing biotin−anti-biotin-labeled pNIPAm-*co*-AAc microparticles (Scheme 2) and nonlabeled pNIPAm-*co*-AAc microparticles (to serve as an internal reference/control). These microlenses were then exposed to a PBS-buffered solution of biocytin (as a free antigen), which binds to the paratope of a anti-biotin tethered onto microlenses by displacement of the biotin−anti-biotin pair with free biocytin. The use of biocytin instead of biotin is one of convenience, since biotin has a low solubility in water. Note that the antibody has a similar intrinsic affinity for both biotin and biocytin. However, because the bound antibody−antigen pair is coupled to, and presumably weakened by swelling pressure of, the microgel, this pair can be displaced by free antigen.[18] This competitive binding results in disruption of biotin−anti-biotin cross-links at the microlens outer surface and, thus, local swelling of the microlens, which induces a decrease in the microlens focusing power. In this scheme, projected images through the microlenses are characterized as lens "on" or "off" as a function of the microgel deswelling/swelling, respectively. The image being projected in these studies is a white square, positioned as indicated in Scheme 1. In this setup, we have focused the microscope such that the square is in focus in the microlens off-state, and when the microlens focal length decreases (microlens on-state) the square image becomes minified to the center of the microlens, thus producing what appears to be a bright spot at the image center. The bright periphery of the image is apparently

(22) Hermanson, G. T. *Bioconjugate Techniques*, 1st ed.; Academic Press: San Diego, CA, 1996; Vol. 1.

Scheme 1. Inverted Light Microscopy Setup Used for Imaging Hydrogel Microlenses[a]

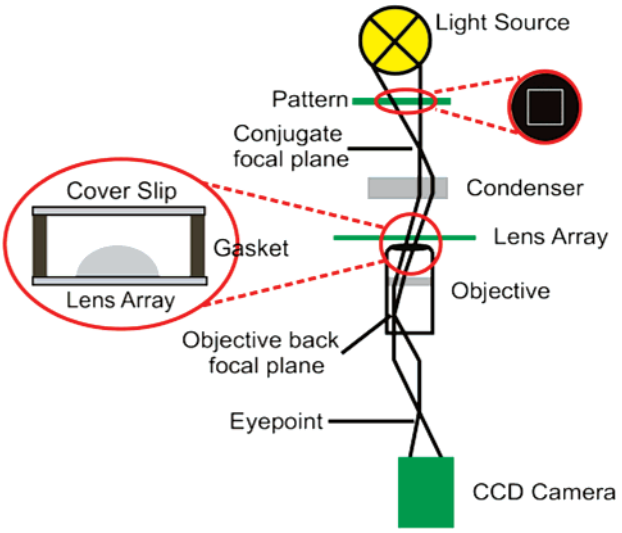

[a] Lenses at the imaging plane move the objective back focal plane to the eyepoint, thus bringing the square pattern positioned near the source into focus at the CCD image plane.

Scheme 2. General Concept for Response Rate Study on Label-Free Sensing by Use of Bioresponsive Hydrogel Microlens Construct[a]

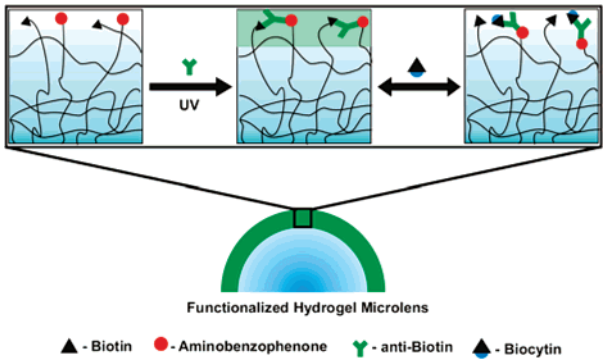

[a] pNIPAM-*co*-AAc microgels are functionalized with biotin and ABP via EDC and DCC, respectively, and then assembled as microlenses on an APTMS-functionalized glass substrate (top left). The microlenses are incubated with polyclonal anti-biotin and then exposed to UV light for photochemical cross-linking of the anti-biotin to the microlenses (top center). The microlenses are exposed to a solution of biocytin buffered in PBS, and, consecutively, their optical properties are monitored via brightfield optical microscope and CCD camera (top right).

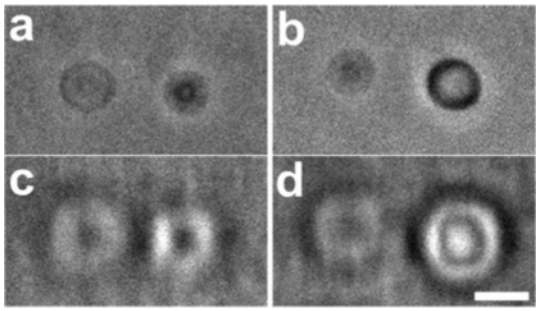

Figure 1. Response of hydrogel microlenses to incubation with polyclonal anti-biotin antibodies. DIC microscopic images of pNIPAm-*co*-AAc hydrogel microlenses (left element in each image) and biotin/ABP functionalized hydrogel microlenses (right element in each image) are shown, (a) before and (b) after incubation with 1 μM anti-biotin. Also shown are projected square-pattern (shown in Scheme 1) images c and d through the hydrogel microlenses under the same conditions as described for images a and b, respectively. The scale bar is 2 μm.

due to a second effective focal length, perhaps due to the compound structure (meniscus + plano convex) of the microlens. Details of the image-forming ability of these microlenses are still a subject of investigation in our group.

The change in focusing power of biotin-modified microlenses as a result of polyclonal anti-biotin binding is shown in Figure 1. Here, we have prepared a microlens assembly containing pNIPAm-AAc microlenses (left element in each image as an internal reference) and biotin/ABP-functionalized pNIPAm-AAc microlenses (right element in each image as the responsive element) in Figure 1a,c. The microlenses were incubated with a 1 μM solution of anti-biotin solution and then irradiated with UV light, allowing for photothetering of anti-biotin to microlens surface (Figure 1b,d). Note that the biotin/ABP + antibody microlens displays a dark circle at the particle periphery in the DIC image (Figure 1b) and also shows changes in the image projection (Figure 1d). However, there is no discernible change in the optical properties of the pNIPAm-*co*-AAc (nonbiotinylated) microlenses after antibody incubation. These results suggest that the biotin/ABP functionalized microlenses deswell by formation of biotin−anti-biotin cross-links at the microlens surface, causing a change in the local refractive index (RI). We will refer to this as the on-configuration.

This change in image fidelity arises from a change in the effective focal length of the microlens between the on- and off-states. To more quantitatively determine the difference in focusing power, we measured the distance between a focusing point of the light source and the fixed surface plane of the glass substrate by using a brightfield microscopy setup. These measurements result in effective focal lengths for the on- and off-states of ~3.1 and 6.2 μm, respectively. It is clear that the bioresponsive microlenses are able to show significant changes (~2-fold decrease in focal length) in the optical properties as a result of antibody binding and the concomitant cross-link formation. Note that the measured focal lengths are determined within the context of our specific microscope setup and therefore represent only the relative change in focusing power. The actual focal lengths of the isolated microlenses may in fact be somewhat different.

To investigate the time-dependent response of the bioresponsive microlenses, they were exposed to the various

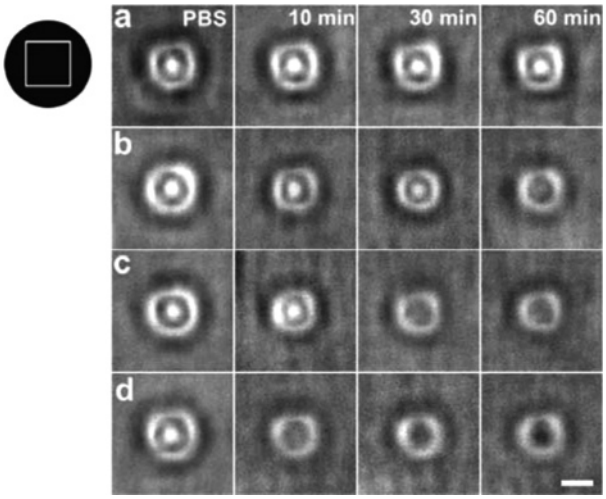

Figure 2. Lens switching times as a function of free biocytin concentration. Projection of a square pattern (shown on top left) through a hydrogel microlens prepared via incubation with 2.0 μM anti-biotin. Biocytin concentrations: (a) 10, (b) 50, (c) 100, and (d) 500 μM. Contact times are indicated at the top of each column, with the initial image in PBS shown in the first column. The scale bar is 2 μm.

antigen concentrations in 10 mM phosphate-buffered saline (PBS), and the image fidelity was monitored over time. Figure 2 shows the behavior of the microlenses as a function of antigen incubation time. The results show that the characteristic time scale for microlens swelling is a function of the solution antigen concentration. As one would expect, the response is rapid (<10 min) under higher antigen concentrations (row d), while low antigen concentrations do not induce swelling on the time scale of this experiment (row a). We interpret these results by considering that hydrogel swelling is induced by displacing a critical number of tethered antibody−antigen binding pairs. The time required for antibody−antigen displacement will be dependent on the intrinsic dissociation rate constant of this pair, the intrinsic association rate between the free antigen and the bound antibody, and the concentration of free antigen. Under the conditions that gave rise to Figure 2, where the bound antibody−antigen concentration is held constant, the free antigen concentration remains the only tunable variable. In light of these results, we expect that the response rate of the microlenses will be related to the microlens sensitivity, which is determined by the number of bound antibody−antigen pairs.

The ability to determine the antigen concentration in both equilibrium and kinetic modes may allow us to apply this behavior to multidimensional antigen sensing. For example, Figure 3 shows the microlens state in response to free antigen as a function of both the exposure time and the tethered antibody concentration. It is interesting to note that the different number of on or off lenses serves to form a response pattern that is a function of the solution antigen concentration [10 μM (left), 50 μM (center), 100 μM (right)]. Such time-evolving patterns may be of use in increasing the ability to discriminate between small differences in antigen concentration and may also increase the dynamic range of such sensor arrays.

The microlens focusing state in response to antigen concentration as a function of time is shown in Figure 4.

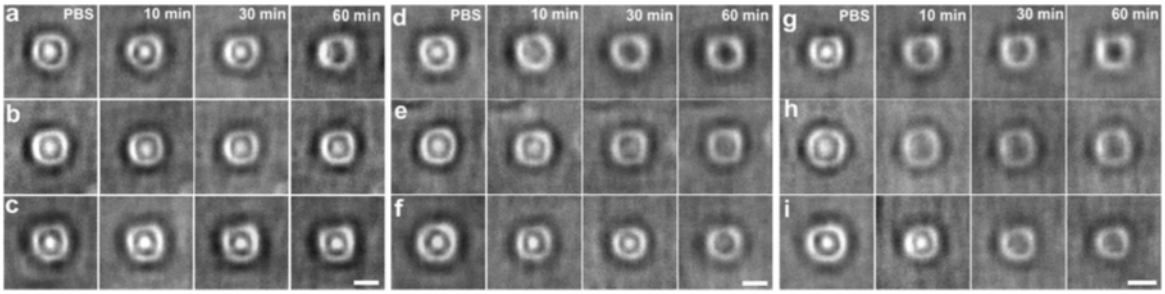

Figure 3. Microlens response as a function of sensitivity (i.e., bound antibody concentration). Projections of the square pattern (shown in Scheme 1) through a microlens incubated and photo-cross-linked in anti-biotin solutions with concentrations of 0.7 μM (top row a, d, g), 1 μM (middle row b, e, h), and 2 μM (bottom row c, f, i) are shown. The number of "on" or "off" lenses was measured as a function of exposure time to various biocytin concentrations [(left (a−c) = 10 μM biocytin, center (d−f) = 50 μM biocytin, right (g−i) = 100 μM biocytin]. Contact times are indicated at the top of each column, with the initial image in PBS shown in the first column. The scale bar is 2 μm.

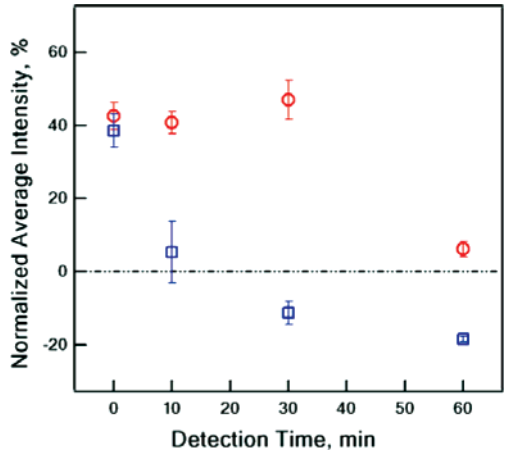

Figure 4. Normalized average intensity of the projected images as a function of lens time. The average intensity of central region (0.55 μm^2) in the projected images was normalized against the background intensity and then determined as a function of free biocytin concentration: (red circles) 50 μM and (blue squares) 500 μM. The error bars represent ± 1σ about the average intensity of four microlens images.

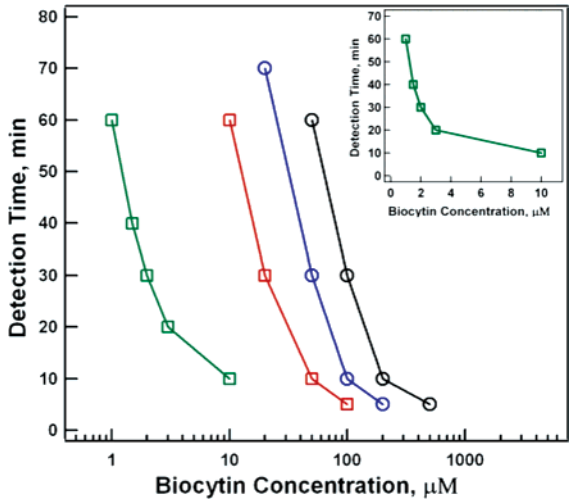

Figure 5. Lens switching rate, measured as a function of free biocytin concentration for microlenses prepared from a range of solution concentrations of anti-biotin. The anti-biotin concentrations used were (green squares) 0.3 μM, (red squares) 0.7 μM, (blue circles) 1.0 μM, and (black circles) 2.0 μM. (Inset) 0.3 μM anti-biotin incubated case with the *x*-axis on a linear scale.

The normalized average percent intensity was determined by subtracting the average background intensity of the captured images from the average intensity of the central region (0.55 μm^2) of the image projected through the microlens. Thus, a positive value can be considered as the lens-on state, where the central region of the projected square image (see Figures 1−3) is brighter than the background. As expected from the images shown in Figure 2b,d, the projected image intensity allows one to distinguish between the lens-off and lens-on states. These results suggest that the bioresponsive microlens response to the target antigen can be monitored by quantitative image analysis as opposed to qualitative inspection of the image fidelity.

As described above, we propose that the response time of the microlenses will be related to the number of antibody−antigen cross-links. This behavior is shown in Figure 5. For these experiments, the sensitivity of the microlenses was modulated by the changing number of antibody−antigen cross-links present on the microlens. The microlenses were then exposed to different concentrations of antigen, after which the microlenses were continually observed on the optical microscope. As expected, the response rates of the microlenses, as measured by determining the time required for the microlens focusing state to completely change, are faster at the higher biocytin concentration than at the lower concentration at a specific antibody−antigen cross-link concentration. Thus, the results clearly show that the time required for lens switching is closely related to both the microlens sensitivity and the solution concentration of the antigen.

Conclusions

We have demonstrated that the response rates of antibody−antigen-modified hydrogel microlenses are strongly tied to the equilibrium sensitivities of those materials. We also show that the sensitivity of each microlens is tunable and can be read-out by simple optical microscopy with image analysis software in quantitative fashion. Finally, we have experimentally measured the effective focal lengths of the hydrogel microlenses by optical microscopy, thereby illustrating that the focal length can change by as much as 2-fold during the transition from the on-state to the off-state. Surface localization of the binding pairs may offer advantages with respect to reversibility and switching speed. Most importantly, the hydrogel microlens construct can be prepared in a simple, rapid, and inexpensive manner and can in principle be generalized to the detection of any substance that can disrupt an affinity pair. Examples aside from the antigen−antibody interactions demonstrated here include protein−protein, DNA−DNA, protein−DNA, protein−ligand, and, enzyme−

inhibitor interactions. However, to demonstrate direct applicability of each of these approaches, optimization of the sensor to the relevant analyte concentrations must be undertaken. Accordingly, our group is presently investigating the sensitivity limits for a number of these interactions. These advantages make this bioresponsive material useful not only for label-free biosensing but also potentially applicable to a variety of other applications such as drug delivery and tissue engineering, where direct responsivity to the surrounding biological environment is advantageous.

Acknowledgment. L.A.L. acknowledges financial support from a Sloan Fellowship and a Camille Dreyfus Teacher−Scholar Award. We thank Professor M. Srinivasarao for helpful discussions during the course of this work.

CM063086P